Chemical Methodologies 8(2024) 351-363

Chemical Methodologies

Journal homepage: http://chemmethod.com

Original Article

Zinc Alginate Beads as an Effective Biosorbent for the Removal of Eosin-B from Aquatic Solutions: Equilibrium, Kinetics, and Thermodynamic Behaviors

Mohsen Samimi*, Khadijeh Amiri

Department of Chemical Engineering, Faculty of Engineering, Kermanshah University of Technology, Iran

ARTICLEINFO

Article history

Submitted: 2024-03-08
Revised: 2024-04-02
Accepted: 2024-05-07

ID: CHEMM-2404-1791
Checked for Plagiarism: Yes
Language check: Yes

DOI: 10.48309/CHEMM.2024.454717.1791

KEYWORDS

Biosorbent
Eosin-B
Isotherms
Kinetics
Thermodynamic parameters
Zinc alginate

ABSTRACT

Spherical alginate-based hydrogels have been applied for environmental pollutants removal from aqueous solutions. In this study, zinc alginate beads were prepared using an ionotropic gelation process. The wet hydrogels prepared in various operational conditions were studied to remove eosin-B dye. The effect of operational variables such as pH, initial concentration of eosin-B, contact time, dose of synthesized hydrogel beads, and environmental temperature on the eosin-B removal process was evaluated. The maximum dye removal efficiency was obtained by zinc alginate biosorbent at pH = 3, contact time of 40 min, and 35 mg of biosorbent dose. The maximum adsorption capacity of zinc alginate beads for eosin-B uptake was 53.48 mg/g of biosorbent. The mechanism, kinetics, isotherms, and thermodynamic studies of eosin-B sorption by zinc alginate hydrogels were investigated. Based on the results, the biosorption process follows pseudo-second-order kinetics. The experimental data of the biosorption process are matched with the Langmuir isotherm model, suggesting that monolayer adsorption plays a vital role in the analyte biosorption. According to the thermodynamic studies, the parameters $\Delta H°$ (+4679.12 $J.mol^{-1}$), $\Delta G°$ (from -173.45 to -499.13 $J.mol^{-1}$), and $\Delta S°$ (+16.284 $J.mol^{-1}.K^{-1}$) confirmed the endothermic, spontaneity and randomness of the biosorption process, respectively. This study shows that zinc alginate can be a suitable biosorbent for removing eosin-B from aqueous solutions.

* Corresponding author: Mohsen Samimi
E-mail: m.samimi@kut.ac.ir

GRAPHICAL ABSTRACT

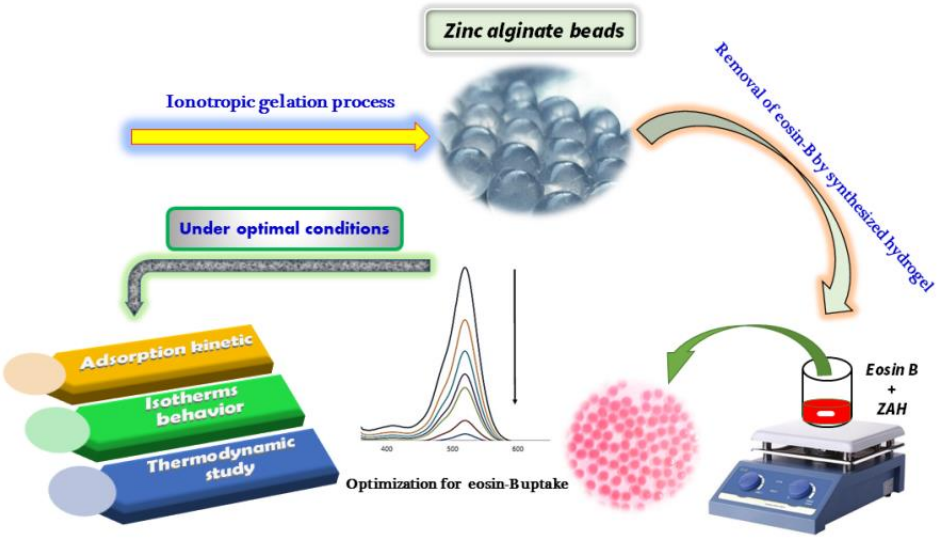

Introduction

With the population growth that has led to the crisis of fresh water shortage, water and wastewater treatment is still one of the concerns of the communities [1]. Industrial activities have also led to a further increase in pollution, which leads to a decrease in water quality [2,3]. Various pollutants such as phenolic compounds [4,5], pesticides [6-8], heavy metals [9-12], agricultural fertilizers, harmful bacteria produced from waste, microplastics, etc. endanger water resources [13-16]. Meanwhile, the effluents of some textile and dyeing industries also contain colored and harmful pollutants [17]. Removing dyes process is often challenging due to their complex aromatic molecular structure and their resistance to decomposition [18,19]. Some dyes in aquatic environments are toxic, carcinogenic, and non-biodegradable, which endangers the survival of aquatic animals and plants, so it is considered as a great threat to human health [20-22]. Eosin-B, an anionic red fluorescent dye belonging to the family of xanthene dyes, has garnered significant attention due to its versatile applications across various fields [23]. Originally developed as a histological stain for biological tissues, eosin-B has evolved to find widespread use in diverse scientific, medical, and industrial applications. Its stability, solubility, and compatibility with different substrates make it a preferred choice for coloring agents in various applications. Eosin-B, obtained from the reaction of bromine with fluorescein, is easily soluble in water and ethanol and is widely used in textile dyeing, ink production, cosmetics coloring, etc. Eosin-B, which is toxic due to its aromatic properties, irritates the eyes, skin, and mucous membranes, and exposure to eosin-B causes skin inflammation and dermatitis [24]. In the past decades, various methods such as physical and chemical methods, coagulation, advanced oxidation, reverse osmosis, adsorption, etc. have been used to remove dyes from aqueous solutions [25,26]. One of the most popular techniques in dye removal is the use of natural adsorbents. In research, hydrogels have been introduced as effective biopolymers in biosorption processes [27]. Hydrogels are three-dimensional polymer networks connected with transverse connections. Due to having hydrophilic functional groups in their structure, hydrogels can hold a large amount of water and aqueous solutions without changing their shape [28]. The presence of special functional groups such as OH, NH_2, COOH, $CONH_2$, and SO_3H in the structure of hydrogels causes the water pollutants uptake. Hydrogel resistance to dissolution comes from the transverse connections between the network chains. Alginate is a natural anionic polysaccharide extracted from brown algae.

This biopolymer consists of α-L-guluronic acid and β-D-mannuronic acid repeated along the chain with an irregular pattern [29]. Alginate-based hydrogels have also been used as adsorbents in the removal of dyes and heavy metals due to biodegradability, cheapness, availability, and hydrophilic properties, in addition to be used in controlled drug release systems [30]. Alginate gel is formed when carboxylate groups interact with divalent or trivalent metal ions [31].

Zinc divalent metal is an antibacterial agent with good thermal stability, which, except for its ionic state, has low toxicity and good biological compatibility [32,33]. This study was conducted to prepare zinc alginate hydrogels (ZAH) for the optimal uptake of eosin-B from aquatic solutions. Furthermore, the dye biosorption kinetics, equilibrium, and thermodynamic behavior of the biopolymer produced in analyte adsorption have been investigated.

Experimental

Materials

Medium sodium alginate (2%-3500 cps) and zinc chloride were obtained from Sigma Aldrich, USA, and eosin-B powder was obtained from Merck, Germany. The stock dye solution was prepared by dissolving 1000 mg of eosin-B dye (chemical formula of $C_{20}H_8Br_2N_2O_9$, molecular weight of 624.06 and λ= 519 nm) in 1000 mL of distilled water, and it was diluted with double distilled water to the desired concentration. The pH value was adjusted by adding 0.1 M NaOH or HCl.

Preparation of ZAH Biosorbent

Zinc chloride salt and sodium alginate powder were dissolved individually in distilled water using a magnetic stirrer (400 rpm at 25 °C) for 1 hour to obtain final solutions of zinc chloride (1500 ppm) and sodium alginate (2% w/v). A certain amount of sodium alginate solution was dripped according to the experimental conditions by a burette with a nozzle tip diameter of 1.2 mm in a container containing 100 mL of zinc chloride solution with a flow rate of 120 ml/min. Finally, spherical ZAH beads in uniform sizes were prepared based on ionotropic gelation through the electrostatic interaction of carboxylic groups between alginate and zinc ions. The precipitated hydrogel beads were collected after 30 min. ZAH beads were kept in distilled water for removal experiments.

Figure 1 displays the spherical ZAH/ eosin-B beads after the dye uptake process. After removing eosin-B, the dye solution was centrifuged at 6000 rpm for 4 min to separate possible solids from the solution. The uptake percentage of eosin-B from the aqueous solution was calculated indirectly by measuring the amount of analyte remaining in the supernatant at the end of the eosin-B biosorption process.

Figure 1: The ZAH/eosin-B beads after the biosorption process

Batch Adsorption Experiments

The ability of ZAH beads for eosin-B uptake was investigated at room temperature in a batch container. For this purpose, certain prepared seeds (50 number) containing 35 mg of alginate were added to 50 mL of eosin-B solution (10-120 mg/L) under a magnetic stirrer for 40 min. The precipitated ZAH biosorbents were collected from the solution after eosin-B uptake. Finally, the concentration of the remaining analyte after centrifugation of the solution was determined using a UV-Vis spectrophotometer. The amount of adsorbed eosin-B per gram of zinc alginate, q_e, is obtained from the following equations:

Eosin-B removal percentage:

$$\frac{C_0-C_e}{C_0} \times 100\% \quad (1)$$

Eosin-B adsorption capacity:

$$q_e = \frac{C_0-C_e}{W} \times V \quad (2)$$

Eosin-B adsorption capacity at a certain time:

$$q_t = \frac{C_0-C_t}{W} \times V \quad (3)$$

Where, C_0 and C_e (mg/L) are the initial and final concentrations of eosin-B, q_e (mg/g) is the dye biosorption capacity, C_t and q_t are the concentration and the adsorption capacity of eosin-B at time t (min) and W (g) and V (L) are the mass of the biosorbent and the volume of the initial solution of eosin-B. Figure 2 illustrates the absorption spectrum of eosin-B at initial concentrations of 1 to 20 mg/L.

The λ_{max} of 519 nm was chosen as the optimal wavelength for conducting additional analytical tests.

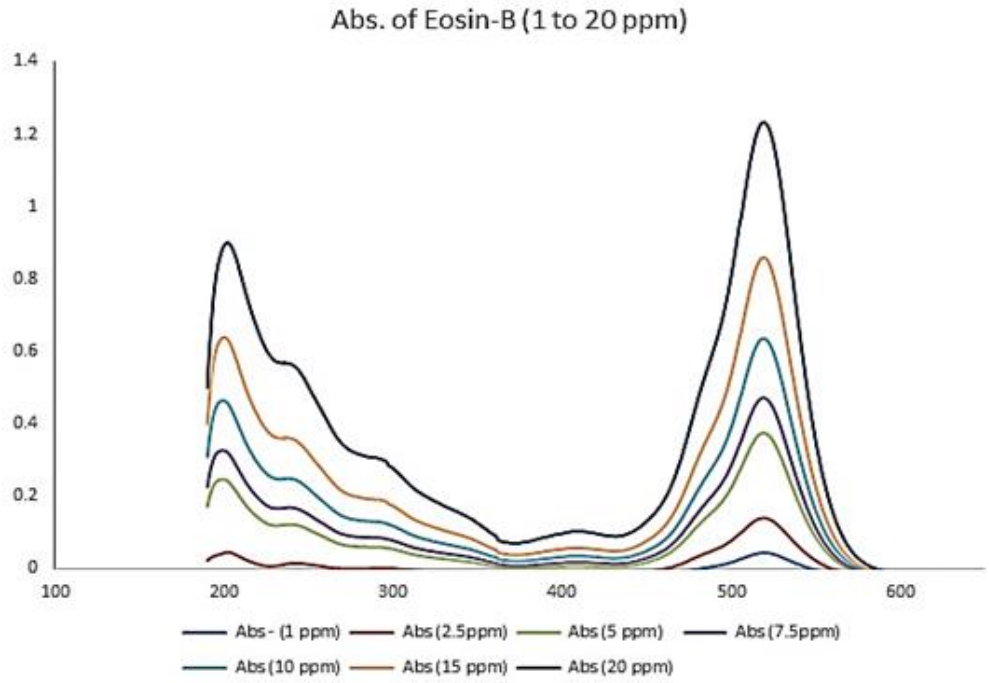

Figure 2: Absorbance spectrum (UV–Vis) of the investigated analyte (eosin-B)

The calibration curve of eosin-B was presented by plotting the intensity of the signal obtained using the UV-Vis spectrometer. According to the acceptable coefficient of determination (R^2 = 0.9912) presented in Figure 3, the absorbance increases linearly with increasing eosin-B concentration. The calibration relationship is given in Equation (4).

$$Abs. = 0.0602\,[Eosin\ B] + 0.0128 \quad (4)$$

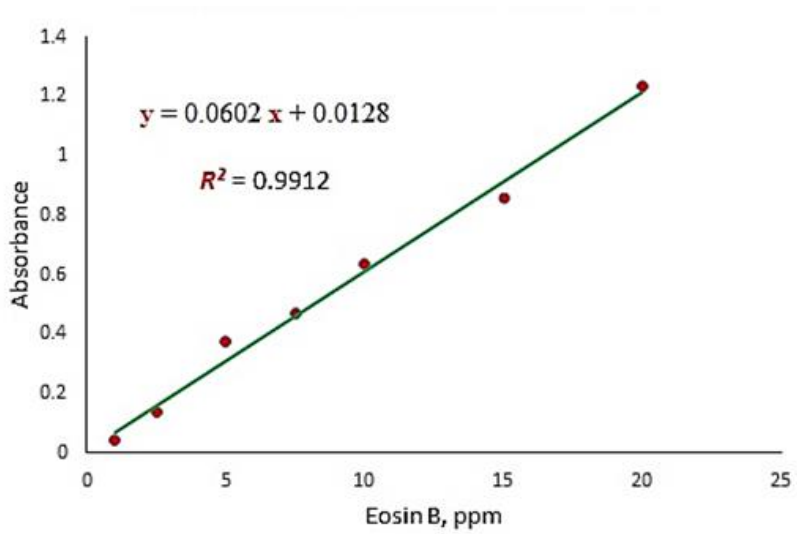

Figure 3: Eosin-B absorbance standard calibration curve

Results and Discussion

Factors Affecting the Eosin-B Removal Process

The initial pH of the solution is one of the factors affecting the dye removal efficiency and causes a change in the structural stability and adsorption intensity of the dye molecules; as a result, it affects the binding site between the adsorbent surface and the solution containing eosin-B. Dye biosorption experiments (50 ml; 50 mg/L; and 20 min at 25) were performed on ZAH beads (50 Numbers containing 35 mg of ZA) at different pH values from 2 to 12. As shown in Figure 4A, with the increase in pH, the removal percentage, and the adsorption capacity of the analyte decreased, which revealed the sensitivity of the adsorbent/analyte surface to the pH value. The increase of excess hydrogen ions at acidic pH the competition between anionic dye and H^+ ions and the enhancement of electrostatic interaction lead to increasing eosin-B adsorption at low pH values. At higher pH, due to the accumulation of OH- on the surface of the adsorbent, which has a negative charge, the electrostatic repulsion of the charge occurs. Consequently, the adsorption of anionic dye molecules decreases. The maximum removal efficiency that also preserves the hydrogel structure was obtained at the optimum pH of 3, which was selected for further experiments. As shown in Figure 4B, the biological adsorption decreased with an increase in the initial concentration of eosin-B. This could occur due to the reduction of access to empty adsorption sites in zinc alginate. The adsorption capacity rises as the dye amount is increased up to 50 mg/L, after which it stabilizes. Appropriate contact time between ZAH beads and eosin-B is an important variable in achieving equilibrium between the biosorbent and dye-containing samples in an aqueous solution, which increases the analyte removal efficiency. Contact times of 5 to 60 min were applied in various experiments of the eosin-B biosorption process to obtain the optimum time.

Figure 4C shows that the adsorption of eosin-B increases with increasing residence time from 5 to 40 min, and this increase is faster due to the availability of empty adsorbent sites in the initial moments of adsorption. After 40 min, analyte adsorption almost reaches equilibrium. The effect of zinc alginate dosage on analyte adsorption was evaluated by varying the amount of hydrogel beads from 300 to 1000 mg/L (15 to 50 mg). As shown in Figure 4D, dye removal increased with increasing hydrogel amount from 300 to 700 mg/L. Likewise, the increase of more than 700 mg/L of biosorbent did not significantly affect the removal percentage and the adsorption capacity of eosin-B decreased. Zinc alginate beads containing 700 mg/L alginate (35 mg alginate) were selected as the optimal biosorbent dosage for further experiments.

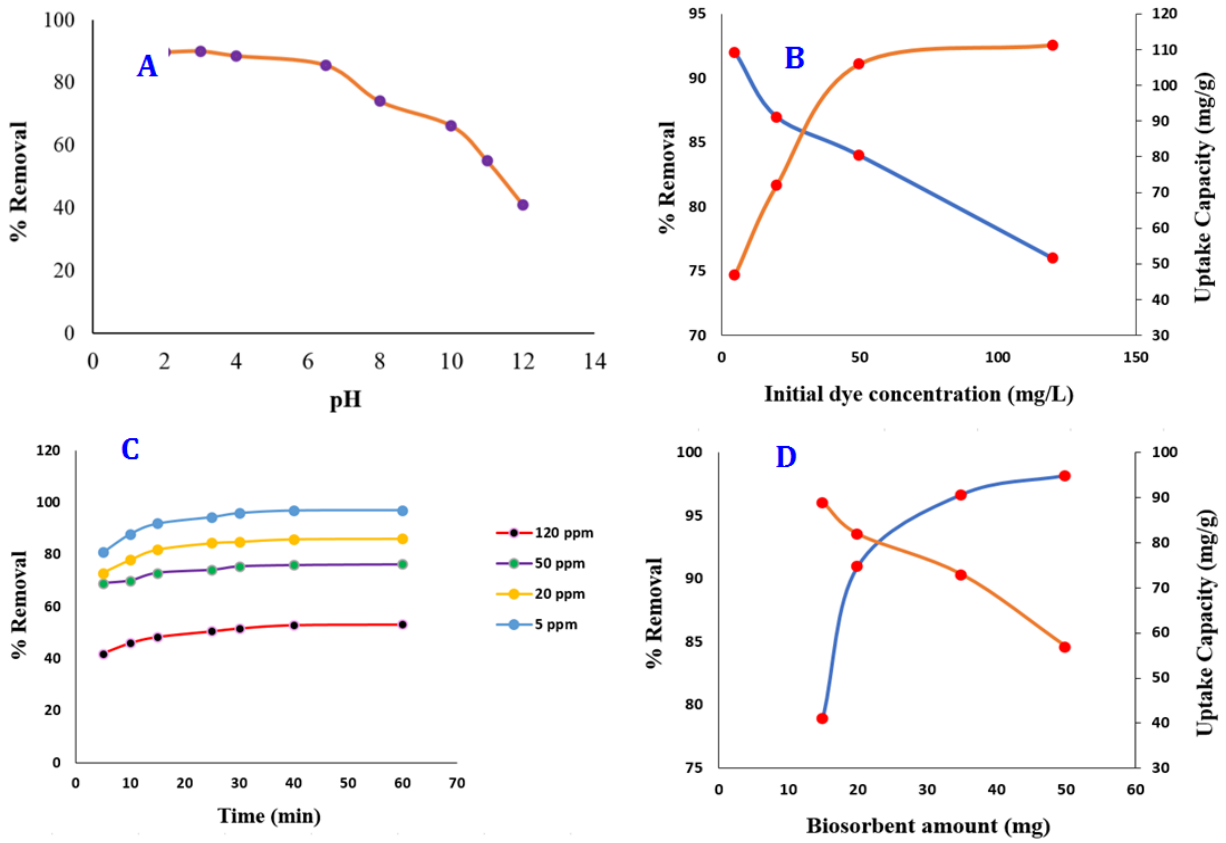

Figure 4: (A) Effect of pH (20 min, 35 mg of biosorbent), (B) initial dye concentration (pH of 3, 40 min, 35 mg of biosorbent), (C) residence time (pH of 3, 35 mg of biosorbent), and (D) hydrogel dosage (pH of 3, 40 min) on eosin-B uptake by ZAH beads from an aquatic solution at 25 °C

Adsorption Isotherms Study

Adsorption isotherms are crucial in examining how analyte molecules are distributed between liquid and solid phases [34]. The experimental data is typically analyzed using three fundamental and straightforward adsorption isotherm models: Freundlich, Langmuir, and Temkin. The relationships of the mentioned isotherm models are briefly presented in Equations (5) to (7), respectively [35,36].

$$\log q_e = \log K_F + \frac{1}{n}\log C_e \quad (5)$$

$$\frac{C_e}{q_e} = \frac{1}{K_L q_{max}} + \frac{C_e}{q_{max}} \quad (6)$$

$$q_e = \beta_T \ln K_T + \beta_T \ln C_e \quad (7)$$

Where, q_{max} and q_e are the maximum monolayer capacity and adsorption capacity in equilibrium. The parameters n and K_F (mg/g) indicate the intensity constant and the Freundlich constant. The Langmuir constants, K_L (L/mg) and C_e, pertain to the affinity of the adsorption sites and the equilibrium concentration of the adsorbed substance [37]. The βT = RT/b (mg/g) is attributed to the heat of adsorption, $b(\mathrm{J.mol^{-1}})$ Temkin's constant, T (K) absolute temperature, $R(8.314\ \mathrm{J.K^{-1}.mol^{-1}})$ is the universal gas constant, and K_T(L/g) is the Temkin constant.

The values of 1/n for the analyte (eosin-B) were between 0 and 1 and showed that the adsorption was acceptable. The Temkin isotherm considers the interaction between adsorbate molecules, resulting in a linear decrease in the heat of adsorption as the surface coverage increases. The effectiveness of models in representing the biosorption process can be evaluated by analyzing the R^2 values [38].

The calculated parameters related to Freundlich, Langmuir, and Temkin isotherms are presented in Table 1. Based on the findings, observed in Figure 5, the Langmuir isotherm model was better than others, which indicates that

monolayer adsorption plays an important role in analyte adsorption by the hydrogel beads.

Table 1: Isotherm parameters in the dye biosorption process by ZAH beads

	Freundlich model			Langmuir model			Temkin model		
	$K_F\left(\frac{mg}{g}\right)$	n	R^2	$q_{max}(\frac{mg}{g})$	$K_L\left(\frac{L}{mg}\right)$	R^2	$K_T(\frac{L}{g})$	$\beta_T(\frac{mg}{g})$	R^2
	5.924	2.072	0.9828	53.476	0.0722	0.9868	1.263	9.593	0.9696

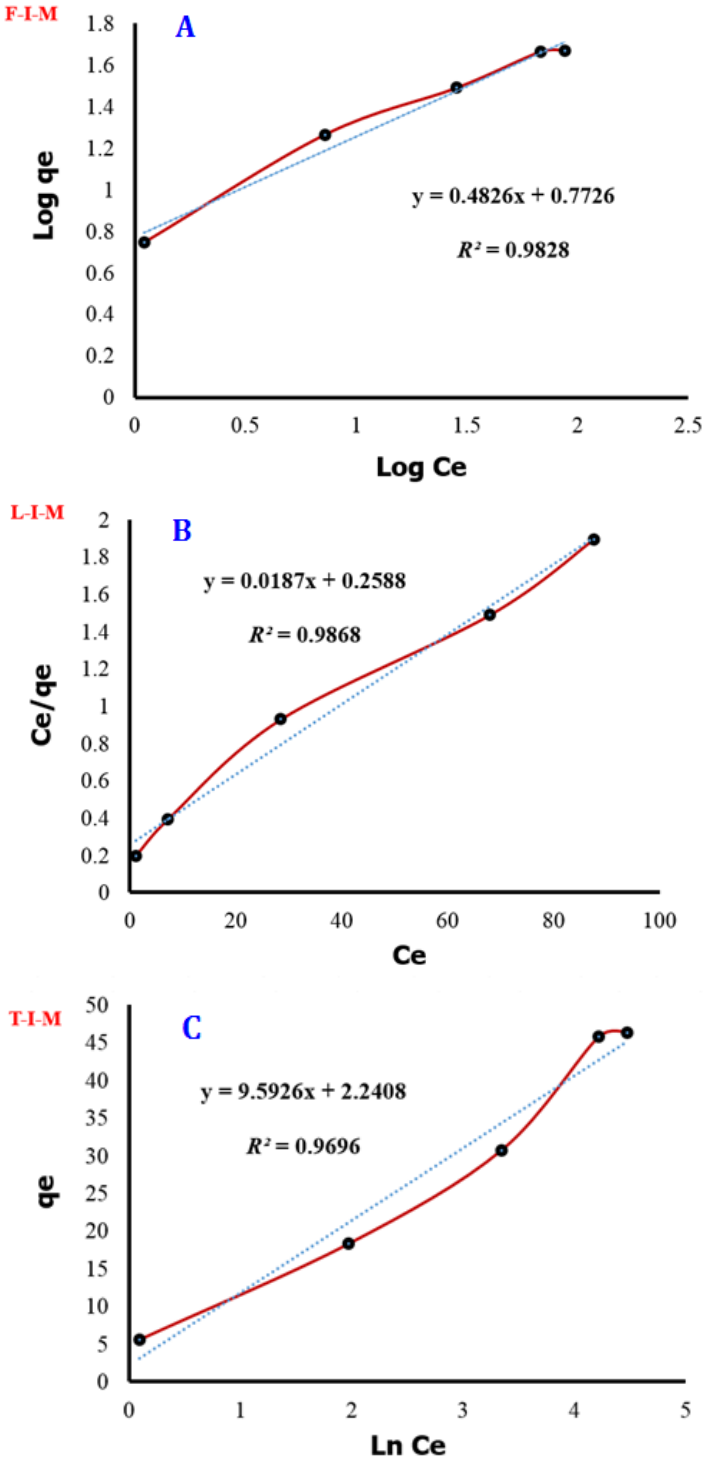

Figure 5: Freundlich (A), Langmuir (B), and Temkin (C) isotherm diagrams for eosin-B adsorption by ZAH

Kinetics and Adsorption Mechanism

The adsorption rate of eosin-B by zinc alginate beads was evaluated using pseudo-first-order, pseudo-second-order and intraparticle diffusion. The linear forms of the aforementioned models are presented in Equations (8) to (10).

$$\ln(q_e - q_t) = \ln q_e - k_1 t \quad (8)$$

$$\frac{t}{q_t} = \frac{1}{k_2 q_e^2} + \frac{t}{q_e} \quad (9)$$

$$q_t = k_p t^{\frac{1}{2}} + C \quad (10)$$

Where, q_e and q_t are the amount of dye adsorbed in the hydrogel structure in the equilibrium state and at a certain time t (min), respectively. Also, $k_2(\frac{g}{mg.min})$ and $k_1(\frac{1}{min})$ are adsorption rate constants. $k_p\ (\frac{mg}{g.min^{\frac{1}{2}}})$ is the intraparticle diffusion constant.

The diagrams of studied kinetics in eosin-B adsorption are shown in Figure 6. As indicated in Table 2, the R^2 value for pseudo-second-order kinetics surpassed that of pseudo-first-order, suggesting that the chemical interaction between the functional groups of ZAH and eosin-B controls the rate of removal.

Thermodynamic Study

The biosorption of eosin-B by ZAH beads was studied at temperatures 298, 308, and 318 K to determine the thermodynamic behavior of the system, both in terms of the physical biosorption process and from the point of view of chemical adsorption. The entropy change (ΔS°), enthalpy change (ΔH°), and Gibbs free energy (ΔG°) were derived using the following equations [39].

$$\Delta G° = \Delta H° - T\Delta S° \quad (11)$$

$$\ln K_c = \frac{\Delta S°}{R} - \frac{\Delta H°}{RT} \quad (12)$$

Where, the equilibrium constant (K_c) is defined as: $K_c = \frac{q_e}{C_e}$. Also, T and R are the temperature and gas constant. The ΔH° and ΔS° amounts were calculated using the values of slope and intercept from the origin obtained from plotting ln Kc against 1/T (Figure 7) and the thermodynamic parameters summarized in Table 3.

The negative value of ΔG° in the investigated temperature range for biosorption of eosin-B shows the spontaneous biosorption process. As listed in Table 3, the Gibbs energy values decrease with increasing temperature. The decrease in ΔG° indicates that the biosorption process is more favorable at higher temperatures. The increase in adsorption capacity at higher temperatures can be related to the enlargement of the pore size or the activation of the adsorbent surface. Likewise, the positive value of ΔH° shows the endothermic nature of biosorption [40]. On the other hand, the positive value of ΔS° also means the stability of adsorption and increasing the degree of randomness of solid/solution collision during the biosorption process. By binding eosin-B molecules to the hydrogel beads, the water molecules that are already attached to the dye are released, and the released molecules in the solution cause an increase in entropy. The positive value of ΔS° indicates the high affinity of the analyte to the biosorbent as well as structural changes during the biosorption process.

Table 2: Kinetics parameters in eosin-B biosorption process by ZAH beads

Kinetic models	Pseudo-first-order			Pseudo-second-order			Intraparticle diffusion		
	$q_e(\frac{mg}{g})$	$k_1(\frac{1}{min})$	R^2	$q_e(\frac{mg}{g})$	$k_2(\frac{g}{mg.min})$	R^2	$k_p\ (\frac{mg}{g.min^{\frac{1}{2}}})$	$C(\frac{mg}{g})$	R^2
	12.26	0.0196	0.868	45.04	0.0078	0.999	1.644	29.81	0.838

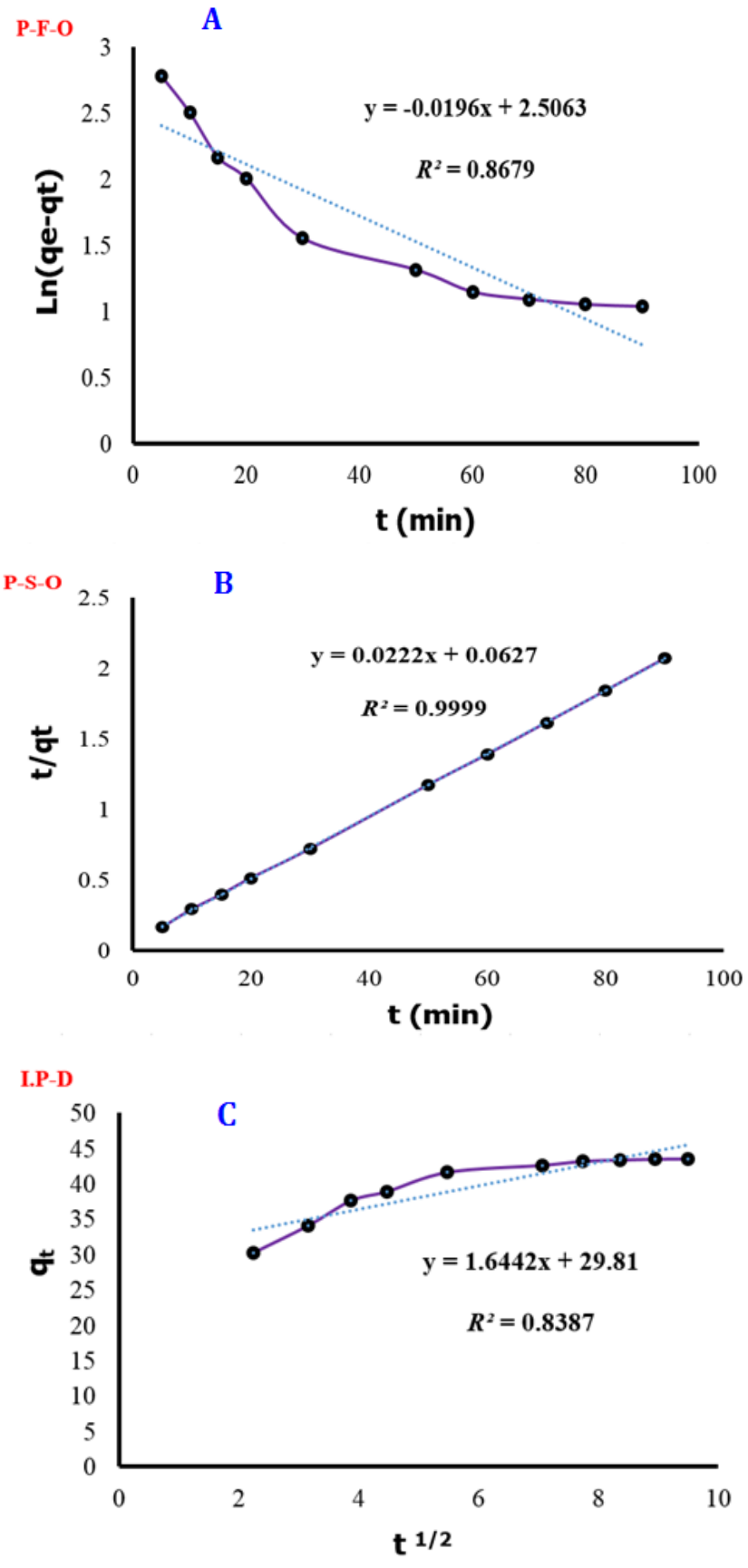

Figure 6: Pseudo-first-order (A), pseudo-second-order (B), and intraparticle diffusion (C) kinetic diagrams for the adsorption of eosin-B using ZAH

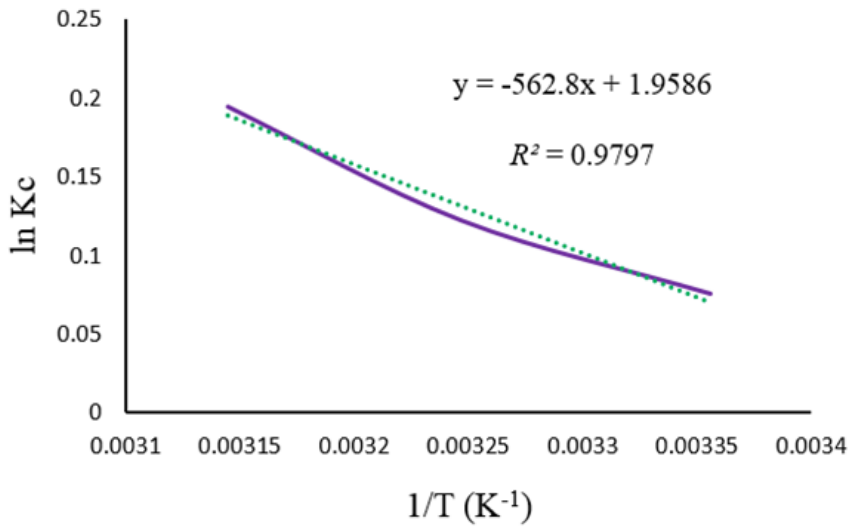

Figure 7: Determination of entropy and enthalpy in the biosorption process of eosin-B by ZAH beads

Table 3: Thermodynamic parameters for adsorption of eosin-B by ZAH beads

$\Delta G°(\frac{J}{mol})$			$\Delta H°(\frac{J}{mol})$	$\Delta S°(\frac{J}{mol.K})$
at: 298 K	**308 K**	**318 K**		
- 173.45	-336.29	-499.13	+4679.12	+16.284

Study of Eosin-B Desorption

The desorption process was studied using water, acetic acid, and diluted hydrochloric acid. The desorption studies revealed the nature of adsorption and the possibility of biosorbent reuse. The weak bonds of eosin-B can be easily broken by water at a neutral pH, while acids such as HCl are used to desorb eosin-B in processes where it is attached to the adsorbent through ion exchange or electrostatic bonds. In the present study, 82% of the adsorbed analyte was desorbed using HC. This indicates the electrostatic nature of eosin-B bonds to ZAH beads.

Conclusion

In the present study, ZAH was prepared based on the ionotropic gelation method, and then its efficiency on eosin-B removal was analyzed. The maximum removal efficiency of eosin-B by zinc alginate biosorbent was obtained at a pH of 3 with the initial dye concentration of 50 mg/L in a contact time of 40 min and 35 mg dose of hydrogels. The mechanism, kinetics, and isotherms of eosin-B adsorption by ZAH were investigated. Based on the results, the Langmuir isotherm model was better than others, which indicates that monolayer adsorption plays an important role in dye biosorption by hydrogel. Examining the thermodynamic behavior, the biosorption process was endothermic, random, and spontaneous. Zinc alginate can be a biocompatible, cheap, and efficient biosorbent for biological dye uptake such as eosin-B.

Acknowledgments

The authors would like to acknowledge the financial support of Kermanshah University of Technology for this research under grant number S/P/T/T/97.

ORCID

Mohsen Samimi
https://orcid.org/0000-0003-3098-7283

References

[1]. Moghadam H., Samimi M., Effect of condenser geometrical feature on evacuated tube collector

basin solar still performance: Productivity optimization using a Box-Behnken design model, *Desalination*, 2022, **542**:116092 [Crossref], [Google Scholar], [Publisher]
[2]. Samimi M., Moghadam H., Modified evacuated tube collector basin solar still for optimal desalination of reverse osmosis concentrate, *Energy*, 2024, **289**:129983 [Crossref], [Google Scholar], [Publisher]
[3]. Samimi M., Mohammadzadeh E., Mohammadzadeh A., Rate enhancement of plant growth using Ormus solution: optimization of operating factors by response surface methodology, *International Journal of Phytoremediation*, 2023, **25**:1636 [Crossref], [Google Scholar], [Publisher]
[4]. Samimi M., Shahriari Moghadam M., Phenol biodegradation by bacterial strain O-CH1 isolated from seashore, *Global Journal of Environmental Science and Management*, 2020, **6**:109 [Crossref], [Google Scholar], [Publisher]
[5]. Gaikwad S.V., Gaikwad M.V., Lokhande P.D., Iodine-DMSO Catalyzed aromatization of Polysubstituted Cyclohexanone derivatives; An efficient methods for the synthesis of polyfunctionized Biaryls derivatives, *Journal of Applied Organometallic Chemistry*, 2021, **1**:1 [Crossref], [Google Scholar], [Publisher]
[6]. Fazeli-Nasab B., Shahraki-Mojahed L., Beigomi Z., Beigomi M., Pahlavan A., Rapid detection methods of pesticides residues in vegetable foods, *Chemical Methodologies*, 2022, **6**:24 [Crossref], [Google Scholar], [Publisher]
[7]. Ahmad F., Mehmood M., A Critical review of photocatalytic degradation of organophosphorus pesticide “parathion” by different mixed metal oxides, *Advanced Journal of Chemistry, Section A*, 2022, **5**:287 [Crossref], [Publisher]
[8]. Khalil M., Noor S., Ahmad Z., Ahmad F., Fate of pakistani exported mango due to its toxicity (heavy metals, pesticides, and other toxic organic components), *Journal of Applied Organometallic Chemistry*, 2023, **3**:86 [Crossref], [Google Scholar], [Publisher]
[9]. Samimi M., Efficient biosorption of cadmium by Eucalyptus globulus fruit biomass using process parameters optimization, *Global Journal of Environmental Science and Management*, 2024, **10**:27 [Crossref], [Google Scholar], [Publisher]
[10]. Pallai D.B., Badekar R.R., Momin K.I., Bondge A.S., Nagargoje G.R., Kadam P.D., Panchgalle S.P., More V.S., Synthesis, spectral and biological studies of Co(II), Fe(II), Ni(II), Cu(II), Pd(II), Mn(II), Hg(II), Cd(II), and Zn(II) complexes derived from benzohydrazide schiff base, *Journal of Applied Organometallic Chemistry*, 2024, **4**:76 [Crossref], [Publisher]
[11]. Ullah R., Ullah T., Khan N., Removal of Heavy Metals from Industrial Effluents using burnt potato peels as adsorbent, *Journal of Applied Organometallic Chemistry*, 2023, **3**:284 [Crossref], [Google Scholar], [Publisher]
[12]. Shayegan H., Safari Fard V., Taherkhani H., Rezvani M.A., Efficient removal of Cobalt(II) ion from aqueous solution using amide-functionalized metal-organic framework, *Journal of Applied Organometallic Chemistry*, 2022, **2**:109 [Crossref], [Google Scholar], [Publisher]
[13]. Samimi M., Shahriari Moghadam M., Optimal conditions for the biological removal of ammonia from wastewater of a petrochemical plant using the response surface methodology, *Global Journal of Environmental Science and Management*, 2018, **4**:315 [Crossref], [Google Scholar], [Publisher]
[14]. Safajou-Jahankhanemlou M., Saboor F.H., Esmailzadeh F., Treatment of tire industry wastewater through adsorption process using waste tire rubber, *Advanced Journal of Chemistry, Section A*, 2023, **6**:85 [Crossref], [Publisher]
[15]. Sardar M.R.I., Hasan F., Alam M.J., Nadim I.H., Mahmud M., A brief review of recent furfural production from lignocellulosic biomass: State of the art of processes, Technologies, and Optimization, *Journal of Applied Organometallic Chemistry*, 2023, **3**:108 [Crossref], [Publisher]
[16]. Ekpan F.D.M., Ori M.O., Samuel H.S., Egwuatu O.P., Emerging technologies for eco-friendly production of bioethanol from lignocellulosic waste materials, *Eurasian Journal of Science and Technology*, 2024, **4**:179 [Crossref], [Publisher]
[17]. Ajani O.O., Bello K.A., Kogo A.A., Synthesis and characterization of acid dyes based on substituted pyridone using metal complexes (1:2) and study of their application on nylon fabrics

(6.6), *Journal of Applied Organometallic Chemistry*, 2023, **3**:61 [Crossref], [Publisher]
[18]. Abegunde S.M., Idowu K.S., Enhanced adsorption of methylene blue dye from water by alkali-treated activated carbon, *Eurasian Journal of Science and Technology*, 2023, **3**:109 [Crossref], [Google Scholar], [Publisher]
[19]. Bashandeh Z., Dehno Khalaji A., Effective removal of methyl green from aqueous solution using epichlorohydrine cross-linked chitosan, *Advanced Journal of Chemistry, Section A*, 2021, **4**:270 [Crossref], [Google Scholar], [Publisher]
[20]. Tavoosi F., Movahedi M., Rasouli N., Preparation and comparison of two different nanocomposite kinds based on MgZnAl-layered double hydroxide for simultaneous removal of cationic and anionic dyes, *Advanced Journal of Chemistry, Section A*, 2021, **4**:32 [Crossref], [Google Scholar], [Publisher]
[21]. Alizadeh K., Khaledyan E., Mansourpanah Y., Novel modified magnetic mesopouros silica for rapid and efficient removal of methylene blue dye from aqueous media, *Journal of Applied Organometallic Chemistry*, 2022, **2**:198 [Crossref], [Publisher]
[22]. Ndung'u S.N., Wanjau R.N., Nthiga E.W., Efficacy of adsorption of congo red dyes from an aqueous media using silicon nitride (Si3N4) adsorbent derived from sand and coffee husk wastes, *Eurasian Journal of Science and Technology*, 2024, **4**:253 [Crossref], [Google Scholar], [Publisher]
[23]. Mahdavi R., Talesh S.S.A., Enhancement of ultrasound-assisted degradation of Eosin B in the presence of nanoparticles of ZnO as sonocatalyst, *Ultrasonics sonochemistry*, 2019, **51**:230 [Crossref], [Google Scholar], [Publisher]
[24]. Bahramifar N., Tavasolli M., Younesi H., Removal of eosin Y and eosin B dyes from polluted water through biosorption using Saccharomyces cerevisiae: Isotherm, kinetic and thermodynamic studies, *Journal of Applied Research in Water and Wastewater*, 2015, **2**:108 [Google Scholar], [Publisher]
[25]. Katheresan V., Kansedo J., Lau S.Y., Efficiency of various recent wastewater dye removal methods: A review, *Journal of Environmental Chemical Engineering*, 2018, **6**:4676 [Crossref], [Google Scholar], [Publisher]
[26]. Kavade R.J., Khanapure R.G., Gawali U.S., Patil, A.A., PatilS.V., Degradation of methyl orange under visible light by ZnO-polyaniline nanocomposites, *Journal of Applied Organometallic Chemistry*, 2022, **2**:89 [Crossref], [Google Scholar], [Publisher]
[27]. Samimi M., Moeini S., Optimization of the Ba+ 2 uptake in the formation process of hydrogels using central composite design: Kinetics and thermodynamic studies of malachite green removal by Ba-alginate particles, *Journal of Particle Science and Technology*, 2020, **6**:95 [Crossref], [Google Scholar], [Publisher]
[28]. Moghadam H., Samimi M., Samimi A., Khorram M., Electrospray modeling of highly viscous and non-Newtonian liquids, *Journal of Applied Polymer Science*, 2010, **118**:1288 [Crossref], [Google Scholar], [Publisher]
[29]. Samimi M., Validov S., Characteristics of pDNA-loaded chitosan/alginate-dextran sulfate nanoparticles with high transfection efficiency, *Romanian Biotechnological Letters*, 2018, **23**:13996 [Crossref], [Google Scholar]
[30]. Khorram M., Samimi M., Samimi A., Moghadam H., Electrospray preparation of propranolol-loaded alginate beads: Effect of matrix reinforcement on loading and release profile, *Journal of Applied Polymer Science*, 2015, **132** [Crossref], [Google Scholar], [Publisher]
[31]. Samimi M., Mohadesi M., Size estimation of biopolymeric beads produced by electrospray method using artificial neural network, *Particulate Science and Technology*, 2023, **41**:371 [Crossref], [Google Scholar], [Publisher]
[32]. Hu C., Lu W., Mata A., Nishinari K., Fang Y., Ions-induced gelation of alginate: Mechanisms and applications, *International Journal of Biological Macromolecules*, 2021, **177**:578 [Crossref], [Google Scholar], [Publisher]
[33]. Ehzari H., Amiri M., Safari M., Samimi M., Zn-based metal-organic frameworks and p-aminobenzoic acid for electrochemical sensing of copper ions in milk and milk powder samples, *International Journal of Environmental Analytical Chemistry*, 2022, **102**:4364 [Crossref], [Google Scholar], [Publisher]

[34]. Samimi M., Safari M., TMU-24 (Zn-based MOF) as an advance and recyclable adsorbent for the efficient removal of eosin B: Characterization, equilibrium, and thermodynamic studies, *Environmental Progress & Sustainable Energy*, 2022, **41**:e13859 [Crossref], [Google Scholar], [Publisher]

[35]. Rostamzadeh Mansour S., Sohrabi-Gilani N., Nejati P., Synthesis and characterization of a nanomagnetic adsorbent modified with Thiol for magnetic and investigation of its adsorption behavior for effective elimination of heavy metal ions, *Advanced Journal of Chemistry, Section A*, 2022, **5**:31 [Crossref], [Google Scholar], [Publisher]

[36]. Samimi M., Shahriari-Moghadam M., The Lantana camara L. stem biomass as an inexpensive and efficient biosorbent for the adsorptive removal of malachite green from aquatic environments: kinetics, equilibrium and thermodynamic studies, *International Journal of Phytoremediation*, 2023, **25**:1328 [Crossref], [Google Scholar], [Publisher]

[37]. Aljeboree A.M., Salah O.H., Altimari U.S., Aljanabi A.A., Alkaim A.F., Highly efficient adsorption of pharmaceutical compounds on sunflower seed shell derived porous carbon, *Advanced Journal of Chemistry, Section A*, 2024, **7**:295 [Crossref], [Publisher]

[38]. Samimi M., Moghadam H., Investigation of structural parameters for inclined weir-type solar stills, *Renewable and Sustainable Energy Reviews*, 2024, **190**:113969 [Crossref], [Google Scholar], [Publisher]

[39]. Asadullah M., Ain Q.u., Ahmad F., Investigation of a low cost, stable and efficient adsorbent for the fast uptake of Cd (II) from aqueous media, *Advanced Journal of Chemistry, Section A*, 2022, **5**:345 [Crossref], [Google Scholar], [Publisher]

[40]. Minjibir S.A., Ladan M., Corrosion inhibition potential of prosopis juliflora leaves extract on mild steel in H_2SO_4 solutions, *Advanced Journal of Chemistry, Section A*, 2023, **6**:311 [Crossref], [Publisher]

Use your device to scan and read the article online

HOW TO CITE THIS ARTICLE

M. Samimi, K. Amiri. Zinc Alginate Beads as an Effective Biosorbent for the Removal of Eosin-B from Aquatic Solutions: Equilibrium, Kinetics, and Thermodynamic Behaviors. *Chem. Methodol.*, 2024, 8(5) 351-363

DOI: https://doi.org/10.48309/CHEMM.2024.454717.1791

URL: https://www.chemmethod.com/article_195714.html